P3.5

Derivation of Improved Surface and TOA Broadband Fluxes Using CERES-derived Narrowband-to-Broadband Coefficients

Mandana M. Khaiyer*, David.R.Doelling, Pui K. Chan, Michele L. Nordeen, Rabindra Palikonda, Yuhong Yi
Analytical Services & Materials Inc., Hampton, VA

Patrick Minnis
Atmospheric Sciences, NASA-Langley Research Center, Hampton, VA

1. INTRODUCTION

Satellites can provide global coverage of a number of climatically important radiative parameters, including broadband (BB) shortwave (SW) and longwave (LW) fluxes at the top of the atmosphere (TOA) and surface. These parameters can be estimated from narrowband (NB) Geostationary Operational Environmental Satellite (GOES) data, but their accuracy is highly dependent on the validity of the narrowband-to-broadband (NB-BB) conversion formulas that are used to convert the NB fluxes to broadband values. The formula coefficients have historically been derived by regressing matched polar-orbiting satellite BB fluxes or radiances with their NB counterparts from GOES (e.g., Minnis et al., 1984). More recently, the coefficients have been based on matched Earth Radiation Budget Experiment (ERBE) and GOES-6 data (Minnis and Smith, 1998). The Clouds and the Earth's Radiant Energy Budget (CERES see Wielicki et al. 1998)) project has recently developed much improved Angular Distribution Models (ADM; Loeb et al., 2003) and has higher resolution data compared to ERBE. A limited set of coefficients was also derived from matched GOES-8 and CERES data taken on Topical Rainfall Measuring Mission (TRMM) satellite (Chakrapani et al., 2003; Doelling et al., 2003).

The NB-BB coefficients derived from CERES and the GOES suite should yield more accurate BB fluxes than from ERBE, but are limited spatially and seasonally. With CERES data taken from *Terra* and *Aqua*, it is now possible to derive more reliable NB-BB coefficients for any given area. Better TOA fluxes should translate to improved surface radiation fluxes derived using various algorithms. As part of an ongoing effort to provide accurate BB flux estimates for the Atmospheric Radiation Measurement (ARM) Program, this paper documents the derivation of new NB-BB coefficients for the ARM Southern Great Plains (SGP) domain and for the Darwin region of the Tropical Western Pacific (DTWP) domain.

2. DATA AND METHODOLOGY

GOES-8 data from April 2000 - March 2003 are used for the SGP, while GOES-9 data taken from June 2004 through May 2005 are analyzed for the DTWP domain. The DTWP domain covers 0°N – 17°S, 125°E – 136°E, while SGP domain covers 32°N-42°N,

91°W - 105°W. All GOES data are calibrated against *Terra* Moderate Resolution Imaging Spectroradiometer data as in Nguyen et al. (2006).

The BB fluxes from the *Terra* CERES FM-1 or FM-2 scanner are matched with the GOES data as follows. The CERES SW and LW fluxes from the 20-km Single Scanner Footprint TOA/Surface Fluxes and Clouds product (SSF; Geier et al, 1999). The SSF footprint data are averaged into a 1° gridded product, the Monthly Gridded Surface Fluxes and Clouds (SFC). The CERES FM-1 or 2 SFC fluxes (cross-track mode only) are matched to GOES 1° gridded narrowband fluxes averaged over a 1° grid within ±15 minutes at viewing zenith angles less than 65° for CERES and 70° for GOES.

Rapid Update Cycle (RUC) model analyses provide vertical profiles of temperature and humidity for the SGP analyses. Meteorological Ozone and Aerosol atmospheric profiles from CERES were used for DTWP processing.

The application of the new ADMs requires determination of the cloud properties for a given scene. The Visible Infrared Solar Split-Window Technique (VISST; Minnis et al., 1995) uses 0.65, 3.9, 11 and 12-μm radiances to derive cloud properties from GOES-8, 9, 10, and 12 data at a nominal pixel resolution of 4 km (Minnis et al., 1998; Phan et al., 2004). ADMs, selected according to the cloud conditions, are used to estimate VIS (0.65-μm) albedos and IR (10.7-μm) fluxes from the NB radiances. VISST processing is done for the expanded TWP region from 10°N – 10°S and 120°E to 180°; the SGP domain processing covers 32°N-42°N, 91°W - 105°W. Validation is performed using GOES-10 and 12 data over the SGP.

The NB-BB coefficients are determined by regressing the GOES NB data against their CERES counterparts using the following equations:

$$A_{bb} = a_0 + a_1 A_{nb} + a_2 A_{nb}^2 + a_3 \ln(1/\mu_o), \qquad (1)$$

where A_{bb} = SW BB albedo, A_{nb} = VIS albedo, μ_o = cos(SZA), and

$$OLR_{bb} = b_0 + b_1 L_{nb} + b_2 L_{nb}^2 + b_3 L_{nb} \ln(RH), \qquad (2)$$

where OLB_{bb} = LW BB flux, L_{nb} = IR flux, and RH = column-weighted relative humidity.

3. RESULTS

Figure 1 shows a scatterplot of the GOES NB albedos and fluxes derived over the SGP domain versus *Terra* CERES broadband fluxes. The average CERES broadband albedo for 91,543 cases was 0.285

compared to the average GOES narrowband albedo of 0.305 (Fig. 1a). The regression curves, also plotted, have a very slight dependence on μ_o. The SW albedo increases with μ_o for a given VIS albedo. Overall, the RMS error in the fit is 7.0%. For 156,149 samples, the mean CERES broadband longwave flux is 243.1 Wm^{-2} (Fig. 1b). It corresponds to an average GOES IR flux of 42.2 Wm^{-2}. The RMS error in the fit is 3.5%. The regression coefficients (Ax) listed at plots' lower right and in Table 1 can be used to convert narrowband fluxes to broadband, using (1) for SW and (2) for LW.

Similar correlations were performed for the DTWP to obtain domain-specific NB-BB regression coefficients. However, since the Darwin domain includes both ocean and land, separate fits were made to account for the spectral differences inherent in these two scene types. The SW albedo is typically larger for clear land than for ocean at the same VIS albedo because the ocean albedo is spectrally flat compared to the land albedo which increases with wavelength from 0.65-µm into the near infrared. Thus, two different fits are needed. Although LW flux land-ocean spectral differences are not as large, some significant differences can occur due to surface emissivity and RH differences. Over the DTWP, column-weighted relative humidity varies greatly between the ocean and the dry Australian continent.

Table 1. Summary of coefficients for the SGP and Darwin new narrowband-to-broadband fits.

	A0	A1	A3	A4
G8 LW	79.02	5.84	-0.02266	-0.25916
G9 LW Ocn	73.03	5.68	-0.00902	-0.36570
G9 LW Lnd	51.31	7.55	-0.03362	-0.41921
G8 SW	0.0657	0.6872	0.03621	0.01586
G9 SW Ocn	0.0380	0.8094	-0.03468	0.04838
G9 LW Lnd	0.0474	0.7806	-0.01435	0.02606

Figure 2 depicts the fits for the DTWP ocean cases. For 11,856 broadband albedo matches (Fig. 2a), the average CERES (GOES) values are 0.159 (0.141). The regression fit shows a slightly larger μ_o-dependence than in Fig. 1a, however, the range of observed μ_o is relatively small in this tropical locale. The RMS error in the multiple regression results is 11.8%. The mean CERES (GOES) OLR for 19,941 cases is 256.2 Wm^{-2} (47.7 Wm^{-2}). Less curvature is apparent in the regression lines compared to the SGP primarily because of a lack of very dry cases over the water. The RMS% error is 2.9%. Similar plots for land are not shown, but the average CERES (GOES) flux for 7,174 LW cases is 273.4 Wm^{-2} (52.4 Wm^{-2}). The regression fit yields an RMS error of 3.3%. For 4,150 cases of SW albedo, the average CERES (GOES) values are 0.1832 (0.1684). The RMS error is 6.6%. The regression coefficients derived for the different domains and scene types are summarized in Table 1.
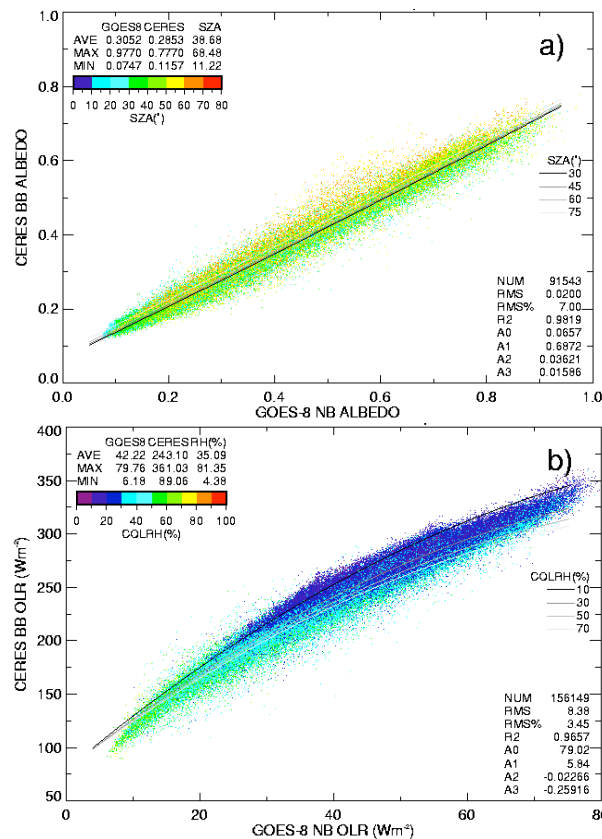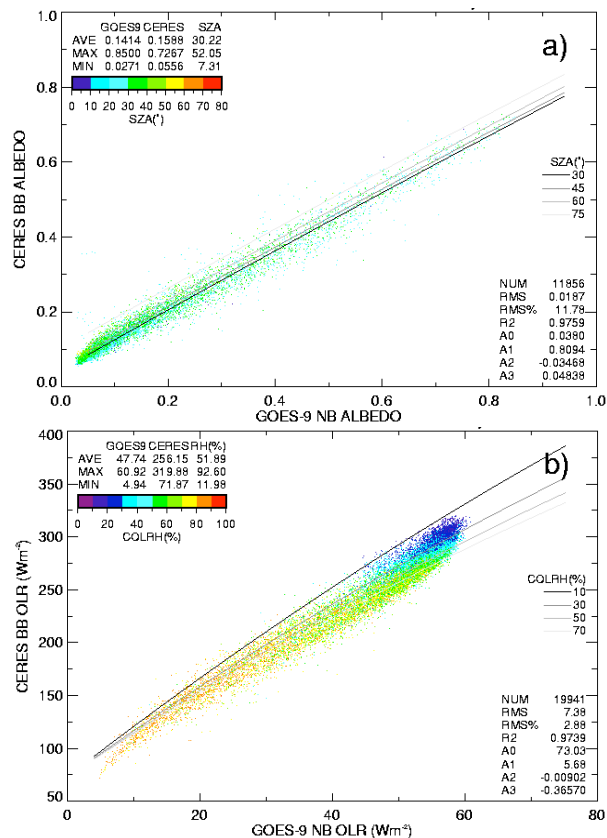

Fig. 1. Scatterplot of NB and BB fluxes for Apr. 2000-Mar. 2003 over the SGP domain using GOES NB and Terra CERES BB a) SW albedos and b) LW fluxes. Colors indicate (a) μ_o or (b) RH.

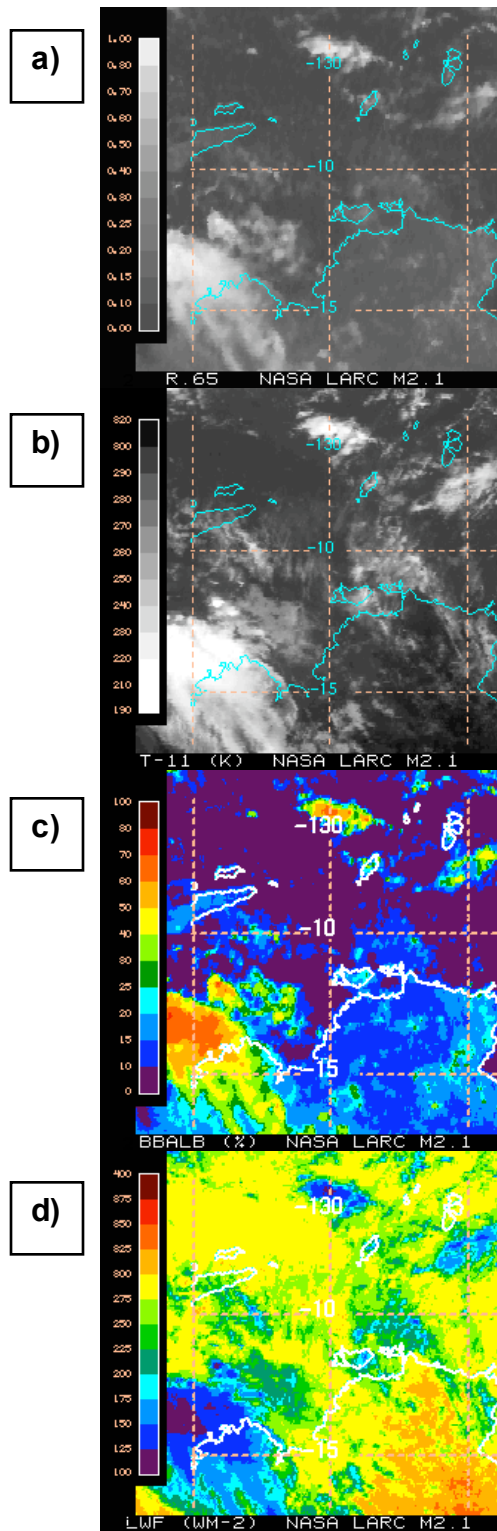Fig. 2. Same as Fig. 1, except for the DTWP domain June 2004 - May 2005 over ocean only.

Fig. 3. GOES-9 derived parameters over the ARM TWP Darwin domain for 0125 UTC Feb 20, 2005 (a) 0.65-µm reflectance, (b) IR brightness temperature, (c) broadband shortwave albedo, (d) broadband longwave flux.

Figure 3 shows the GOES-9 imagery and results for the DTWP at 0125 UTC February 20, 2005, a time coincident with a *Terra* overpass. Indicative of the monsoon season, a deep convective cloud in the lower left corner of the domain exhibits high SW albedos (maxima, 60-70%) and low OLR values (minima, 100-125 Wm⁻²). The ocean albedos are much lower than those over land.

The surface fluxes estimated from satellites are also affected by the accuracy of NB-BB coefficients for deriving TOA flux. Before assessing the impact of the new coefficients, other factors that affect estimates must be examined. VISST cloud properties are used as input to the NASA Langley Parameterized Longwave Algorithm (LPLA; Gupta et al, 1992) that derives upwelling longwave surface flux (UPLW). Skin temperature is the most important input for deriving the surface upwelling longwave flux, so methods deriving it from satellite must be accurate. Figure 4 shows an example of the LPLA algorithm applied to the GOES-12 data over Boulder, Colorado during January 2004 and plotted against surface
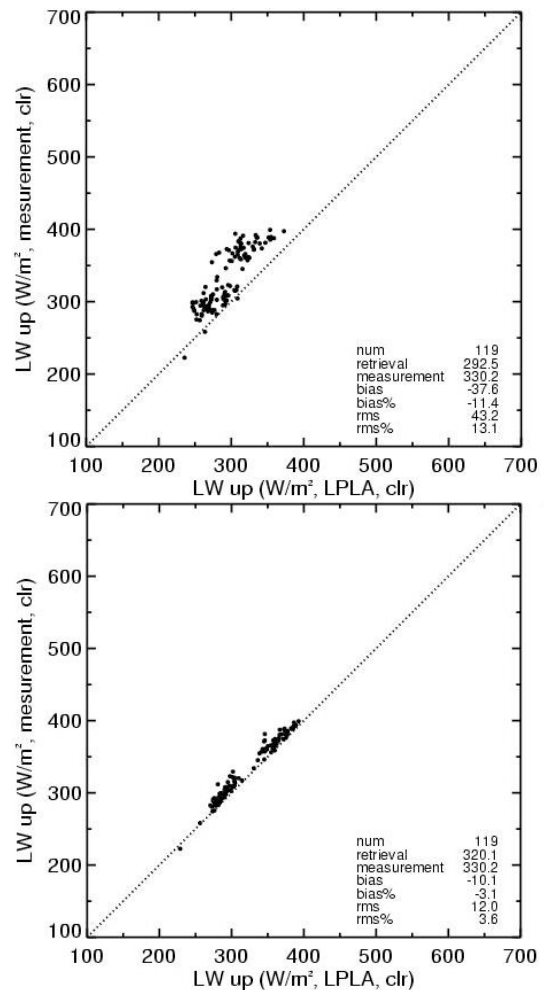

Fig.4 Comparison of clear-sky LPLA and SURFRAD UPLW over Boulder, January 2004, for a) old air-to-skin temperature conversion method and b) correlated-k skin temperature method.
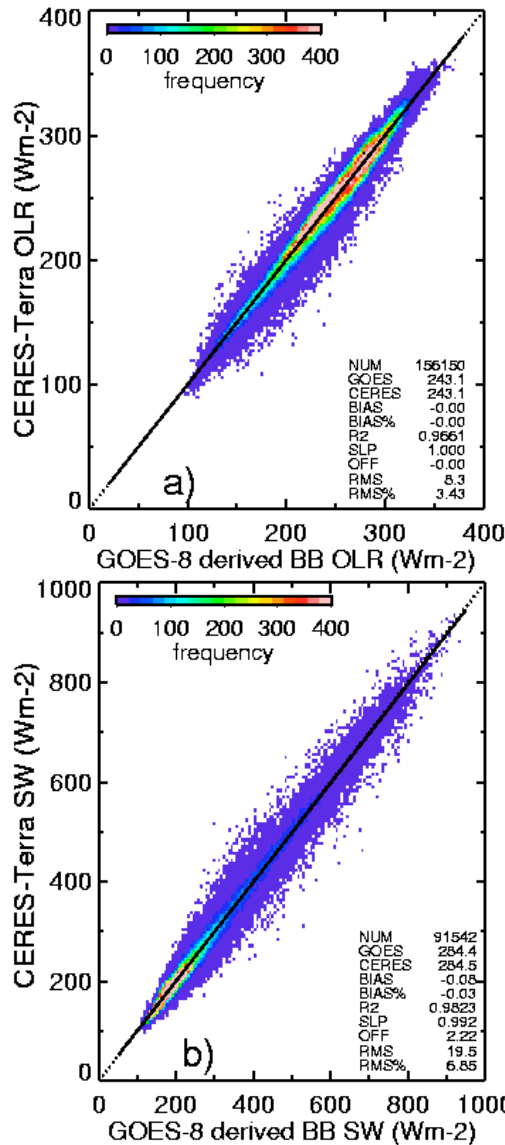
Fig. 5. Comparison of Terra CERES and GOES-8 BB fluxes over the SGP for Apr. 2000- Mar. 2003.

Fig. 6. Same as Fig. 5, except for DTWP for June 2004-May 2005.

measurements from the Surface Radiation Budget Network (SURFRAD). In the past, a simple empirical conversion from air temperature to skin temperature, based on temperatures from the SGP, was employed in derivations of UPLW flux from VISST using LPLA (Fig. 4a). The comparisons of clear-sky UPLW in Fig. 4a yield an RMS error of 13.1% and a bias of -37.6 Wm^{-2}. However, using atmosphere-corrected clear-sky GOES-8 satellite 10.7-µm to obtain skin temperatures (Fig. 4b), the RMS error decreased to 3.6% with a bias of -10.1 Wm^{-2}. The remaining bias may be due to discrepancies in the LW and IR surface emissivities.

4. DISCUSSION

To gauge the effects of these new fits on the data, comparisons can be made of the VISST-derived broadband fluxes to CERES, using both the old and
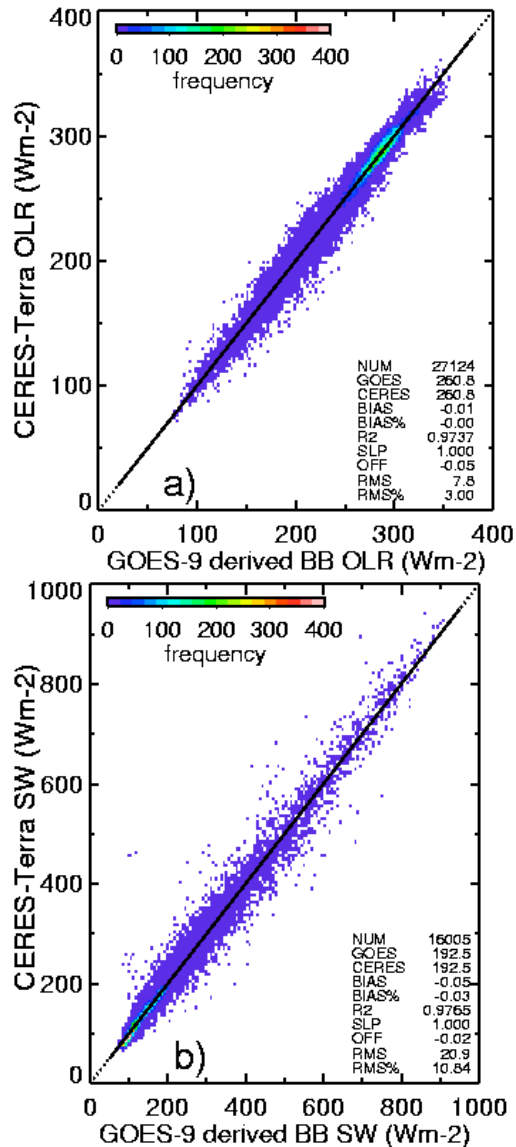
new sets of NB-BB coefficients. Figure 5 compares the GOES-8 SGP TOA broadband fluxes with their CERES counterparts. By applying the NB-BB fit, as well as a third-order linear correction for residuals at the lower end of the scale, both longwave averages are identical at 243.1 Wm^{-2}, with an RMS error of 3.4%. For the shortwave fluxes, the average for CERES (GOES) is 284.5 Wm^{-2} (284.4 Wm^{-2}), so that the bias is very close to 0. The RMS error is 6.9%.

Figure 6 shows how the DTWP GOES-9 TOA broadband fluxes compare to CERES. With a fourth-order linear correction for ocean data, both average longwave fluxes are identical at 260.8 Wm^{-2}, with an RMS error of 3.0%. For the shortwave fluxes, the averages for CERES and GOES are both 192.5 Wm^{-2}, with a bias of 0.1 Wm^{-2}. The RMS error is 10.8%.
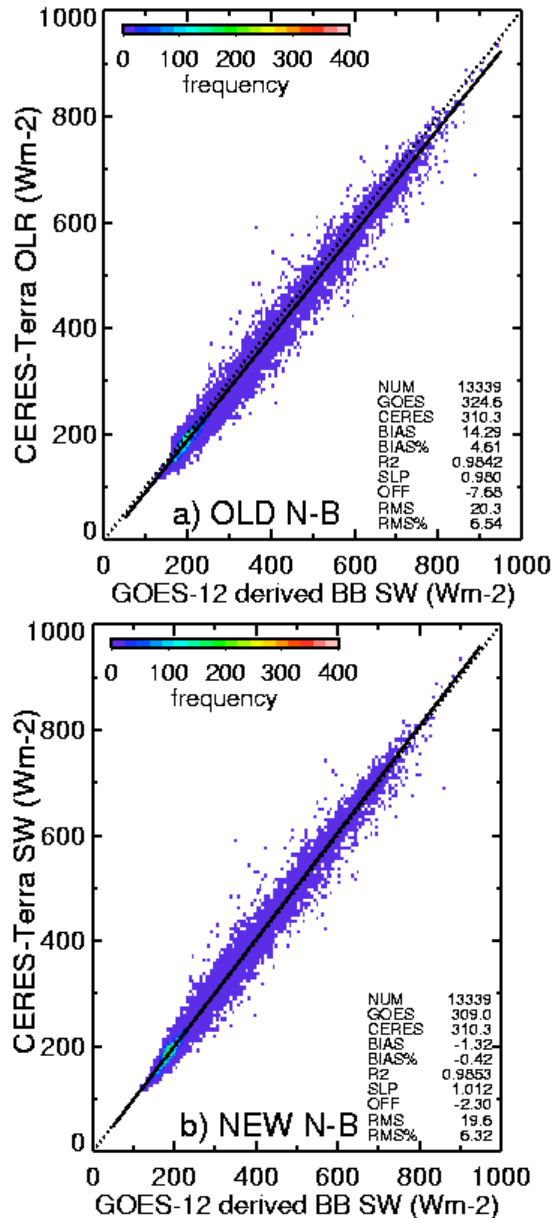
Fig. 7. Validation of GOES-12 SW fluxes over the SGP domain using Terra CERES data from February-May 2005 for (a) old GOES-8-TRMM NB-BB fit and (b) new GOES-8-Terra NB-BB fit.

Table 2. Summary of biases and RMS errors for the SGP and Darwin, old and new narrowband-to-broadband fits. Time periods are denoted as follows: I is April 2000- March 2003, II is June 2004-May 2005, and III is February - May 2005.

	Time Period	Old Bias	Old RMS	New Bias	New RMS
G8 LW	I	1.4%	3.6%	0.0%	3.4%
G9 LW	II	2.4%	3.9%	0.0%	3.0%
G10LW	III	2.9%	3.1%	1.1%	3.0%
G12LW	III	5.1%	3.6%	3.1%	3.6%
G8 SW	I	5.3%	6.9%	0.0%	6.9%
G9 SW	II	-9.5%	13.4%	0.0%	10.8%
G10SW	III	1.8%	6.3%	-2.9%	6.1%
G12SW	III	4.6%	6.5%	-0.4%	6.3%

only -1.3 Wm^{-2} and an rms error of 6.3%. The GOES-10 shortwave results (not shown) improved the RMS error fit, but not the bias. The "before" bias was 5.7 Wm^{-2} with an RMS error of 6.3% changed to an "after" bias of -9.0 Wm^{-2} and RMS of 6.1%. Even so, LW results for both GOES-10 and GOES-12 improved using the new NB-BB fits with a third order correction (not shown). GOES-10 had a bias of 6.8 Wm^{-2} (RMS 3.1%) using the old fit, but improved to a bias of 2.5 Wm^{-2} and a RMS of 3.0% using the new fit. GOES-12 had a "before" bias of 12.1 Wm^{-2} and an RMS error of 3.6%, but an "after" bias of 7.2 Wm^{-2} and an RMS error of 3.6%. The biases and rms errors using old and new NB-BB fits are summarized in Table 2.

5. SUMMARY AND FUTURE WORK

The narrowband-to-broadband fits were recomputed using the most up-to-date satellite information available. GOES-8 and *Terra* were used to derive new NB-BB coefficients for the SGP domain, and GOES-9 and *Terra* were employed for the TWP Darwin domain. SGP fits were for land-only, but Darwin was separated into separate fits for land and ocean. Both domains showed improvement in longwave and shortwave fluxes when the new coefficients were used, as expected.

The new SGP NB-BB coefficients were tested on GOES-10 and GOES-12 as an independent validation. Using the new GOES-8/*Terra* coefficients for GOES-12 improved shortwave and longwave flux biases and rms errors, and improved these parameters for GOES-10 OLR. GOES-10 shortwave fluxes improved in RMS error, but the magnitude of the bias increased.

Correlated-k corrected skin temperatures input to LPLA were shown to improve agreement when compared to SURFRAD data. Surface fluxes could also be improved using the new NB-BB fits, but this is left to future work.

Future work includes performing outside validation for the GOES-9 – *Terra* NB-BB fits. Also, separate NB-BB fits for the wet and dry seasons over the DTWP region will be made. Seasonal fits for the SGP will also be computed to account for any annual cycle. New NB-BB coefficients should be derived separately for GOES-10/*Terra* and GOES-12/*Terra*. Finally, the impact of the improved TOA fluxes from these fits on derived surface fluxes will be assessed.

Although the bias is now close to zero for these cases, that is to be expected since the same cases that created the new NB-BB fit are being used in the validation. In order to see if the NB-BB fit shows improvement, outside validation needs to be performed. GOES-10 and –12 also provide imager data over the SGP for a later time period than the GOES-8 satellite. Shortwave fluxes from Feb 2005 – May 2005 for the GOES-12 satellite are compared in Fig. 7 using the (a) CERES-TRMM NB-BB fits ("OLD N-B") versus the new (b) CERES-Terra fits ("NEW N- B"). The old fits had a bias of 14.3 Wm^{-2} and an RMS error of 6.5%, whereas the new NB-BB fit yields a bias of

References

Chakrapani, V., D.R.Doelling, M.M.Khaiyer, P.Minnis, 2003: New visible to broadband shortwave conversions for deriving albedoes from GOES-8 Over the ARM-SGP. *Proc. 13th ARM Science Team Meeting*, March 31-April 4, Broomfield, CO

Doelling, D.R. M.M.Khaiyer, P.Minnis, 2003: Improved ARM-SGP TOA OLR Fluxes from GOES-8 IR radiances based on CERES data. *Proc. 13th ARM Science Team Meeting*, March 31-April 4, Broomfield, CO

Geier, E.B., R.N. Green, D.P.Kratz, P. Minnis, W.F.Miller, S.K.Nolan, and C.B. Franklin, 2001: Single satellite footprint TOA/surface fluxes and clouds (SSF) collection document. http://asd-www.larc.nasa.gov/ceres/ASDceres.html

Gupta, S.K., Darnell, W.L., and Wilber, A.C.: 1992: A parameterization for longwave surface radiation from satellite data: recent improvements. *J. Appl. Meteor,.***31**, pp. 1361-1367

Loeb, N. G., N. Manalo-Smith, S. Kato, W. F. Miller, S. Gupta, P. Minnis, and B. A. Wielicki, 2003: Angular distribution models for top-of-atmosphere radiative flux estimation from the Clouds and the Earths Radiant Energy System instrument on the Tropical Rainfall Measuring Mission satellite. Part I: Methodology. *J. Appl. Meteorol.*, **42**, 240-265.

Minnis,P. and E.F.Harrison, 1984: Diurnal Variability of Regional Cloud and Clear-Sky Radiative Parameters Derived from GOES Data, Part I: Analysis Method. *Journal of Climate and Applied Meteorology*, **Vol. 23**, pp. 993-1011

Minnis,P. and Smith, W. L., Jr., 1998: Cloud and Radiative Fields Derived from GOES-8 During SUCCESS and the ARM-UAV Spring 1996 Flight Series. *Geophys. Res. Ltrs.,* **25**, pp.1113-1116.

Minnis, P., D. P. Kratz, J. A. Coakley, Jr., M. D. King, D. Garber, P. Heck, S. Mayor, D. F. Young, and R. Arduini, 1995: Cloud Optical Property Retrieval (Subsystem 4.3). "Clouds and the Earth's Radiant Energy System (CERES) Algorithm Theoretical Basis Document, Volume III: Cloud Analyses and Radiance Inversions (Subsystem 4)", *NASA RP 1376 Vol. 3*, edited by CERES Science Team, pp. 135-176.

Minnis, P., D. P. Garber, D. F. Young, R. F. Arduini, and Y. Takano, 1998: Parameterization of reflectance and effective emittance for satellite remote sensing of cloud properties. *J. Atmos. Sci.*, **55**, 3313-3339.

Nguyen, L., P. Minnis, and D. R. Doelling, 2006: Rapid calibration of operational and research meteorological satellite imagers, Part III: Application to geostationary satellite visible channels. Submitted to *J. Atmos. Oceanic Technol.*

Phan, D., D. A. Spangenberg, R. Palikonda, M. M. Khaiyer, M. L. Nordeen, L. Nguyen, and P. Minnis, 2004: Web-based satellite products database for meteorological and climate applications. *Proc. 13th AMS Conf. Satellite Oceanogr. and Meteorol.*, Norfolk, VA, Sept. 20-24, CD-ROM, P8.2.

Wielicki, B. A., et al., 1998: Clouds and the Earth's Radiant Energy System (CERES): Algorithm Overview. *IEEE Trans. Geosci. and Remote Sens.*, **36**, 1127-1141.